# Effect of Chemical Permeation Enhancers on Skin Permeability: In silico screening using Molecular Dynamics simulations

**Rakesh Gupta[1,*], Sridhar Dwadasi[1], Beena Rai[1]** and **Samir Mitragotri[2]**

Physical Science Research Area, Tata Research Development and Design Centre, TCS Research, Tata Consultancy Services, 54B, Hadapsar Industrial Estate, Pune – 411013, India

[2]School of Engineering and Applied Sciences and Wyss Institute, Harvard University

*Corresponding author: gupta.rakesh2@tcs.com

Fax : 91-20-66086399

Phone : 91-20-66086203

## Supporting Information

### S1. Systems used in simulations

**Table S1.** The details of the permeation enhancers and number of the enhancers used in each simulation.

| Name | Functional group | Number of Permeation enhancers (1 w/v) | Number of Permeation enhancers (3 w/v) | Number of Permeation enhancers (5 w/v) |
|---|---|---|---|---|
| Oleic Acid (OLE) | Acid | 15 | 45 | 75 |
| Palmitic Acid (PLA) | Acid | 16 | 48 | 80 |
| Geranic Acid (GRA) | Acid | 25 | 75 | 125 |
| Undecanoic acid (UND) | Acid | 22 | 66 | 110 |
| DMSO (DMS) | DMSO | 57 | 171 | 285 |
| Geraniol (GOL) | Unsaturated alcohol | 27 | 81 | 135 |
| Glyceryl monooleate (GMO) | Glyceryl ester | 12 | 36 | 60 |
| Isopropyl palmiate (ISP) | ester | 14 | 42 | 70 |
| Limonene (LEM) | Unsaturated monoterpene | 31 | 93 | 155 |
| Octylpyrrolidone (OCT) | Pyrrolidone | 21 | 63 | 105 |

## S2. Parameterization of CPEs

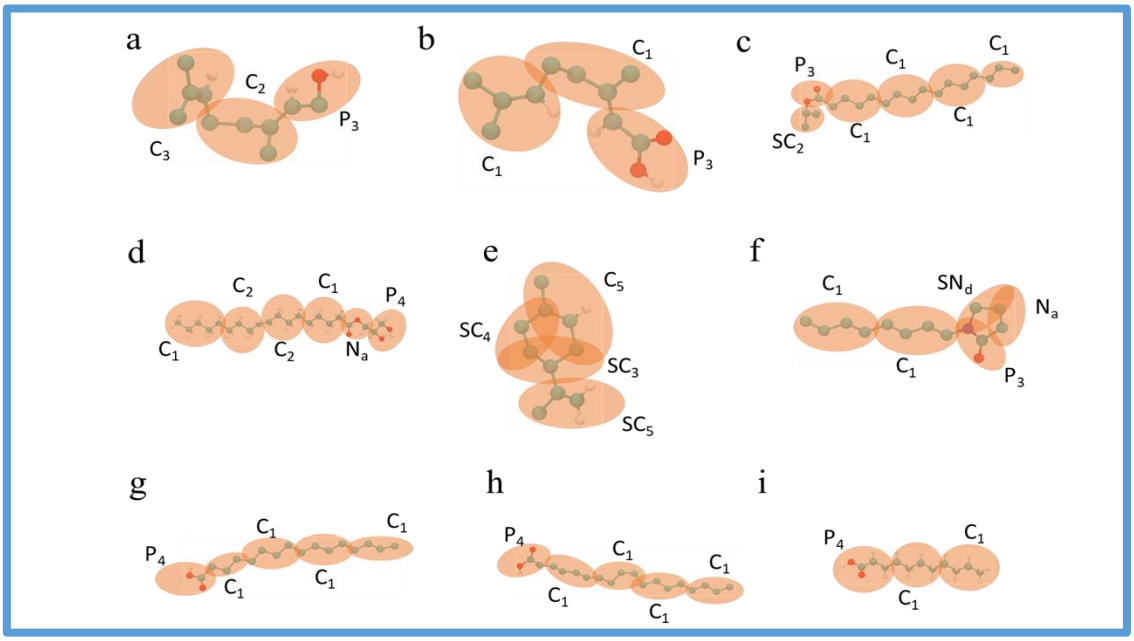


**Figure S1**. Mapping of the molecules into Martini beads (down). a) geraniol, b) geranic acid, c) isopropyl palmitate, d) monoolein, e) limonene, f) n-octyl pyrrolidone, g) palmitic acid, h) oleic acid and i) undecanoic acid. Images were created using VMD software.

The mapping of the atoms into beads was carried out based on MARTINI philosophy. Each bead consists of 3 or 4 atoms, and the bead types were assigned based on the polarity. Bonded parameters of molecules Geraniol, Geranic Acid, Isopropyl Palmitate, Monoolein, Limonene, N-octyl Pyrrolidone were developed by modifying the coarse grain (CG) bonding parameters till a reasonable match of the bonded distributions is obtained as compared to those obtained from atomistic simulations. Also, the bulk density of the CG simulation was compared to the atomistic simulation. All atom simulations, with atleast 300 molecules were carried out for 30 ns and the trajectories were sampled to obtain bond and angle distributions and the bulk density. CG simulations with atleast 300 molecules (number equal to those taken in all atom simulations) were run for 10 ns with a time step of 25 fs, from which the bond and angle distributions and bulk density were obtained. The parameterization of bond parameters was quite straight forward in structures without a ring, but was tricky with ring containing structures (limonene and N-octyl pyrrolidone). The bonded parameters for limonene were taken from those of tyrosine as given in the martini amino acids files [1, 2].

Figures S1-S4 show the comparison of bond and angle distributions obtained from CG (martini) simulations and all atom simulations. These are in reasonable agreement. It should

be kept in mind that in coarse graining, we may not get an exact match with atomistic distributions. Care should be taken that the bonds/angles do not get too rigid. Thus in a few cases (Ex: Fig S1 b1), it can be seen that the distributions match in mean position while the probability may not be as steep. These values gave us reasonable match with bulk density as reported in the main text. Table s1 gives the bonded parameters of the six molecules.

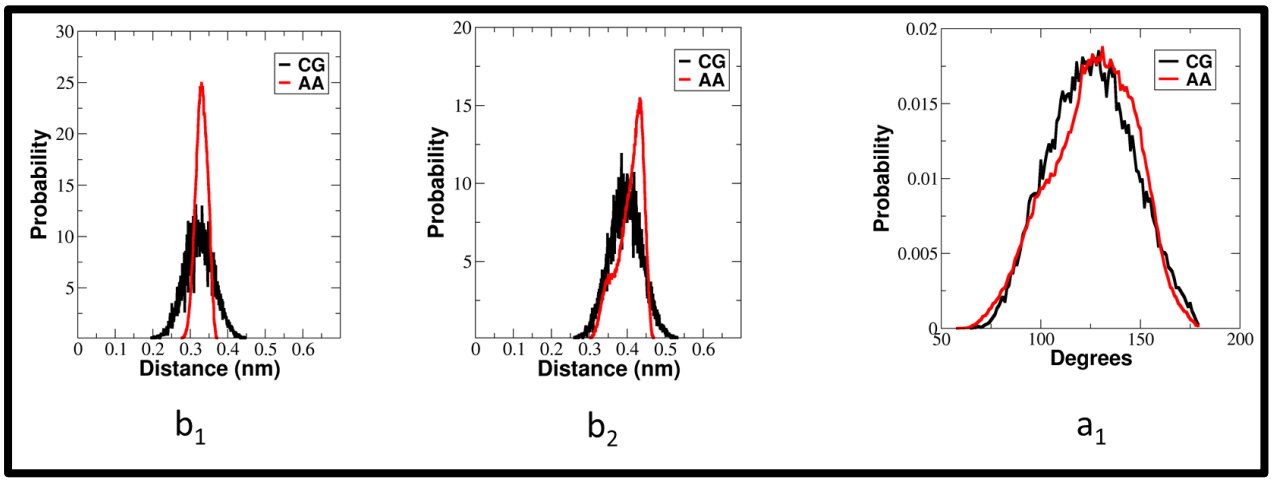


**Figure S2**. Bond and angle distributions for Geraniol.

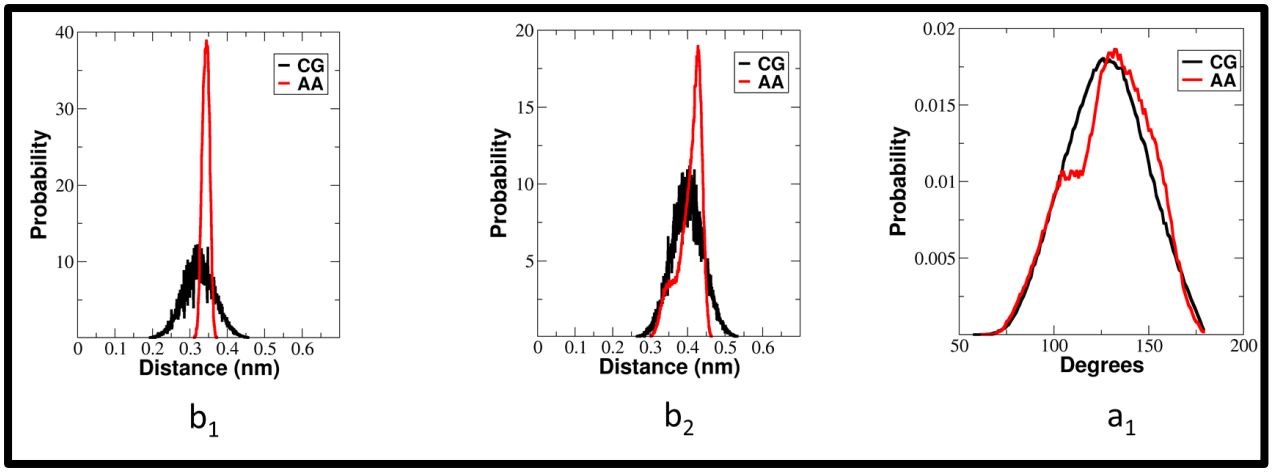


**Figure S3.** Bond and angle distributions for Geranic Acid.

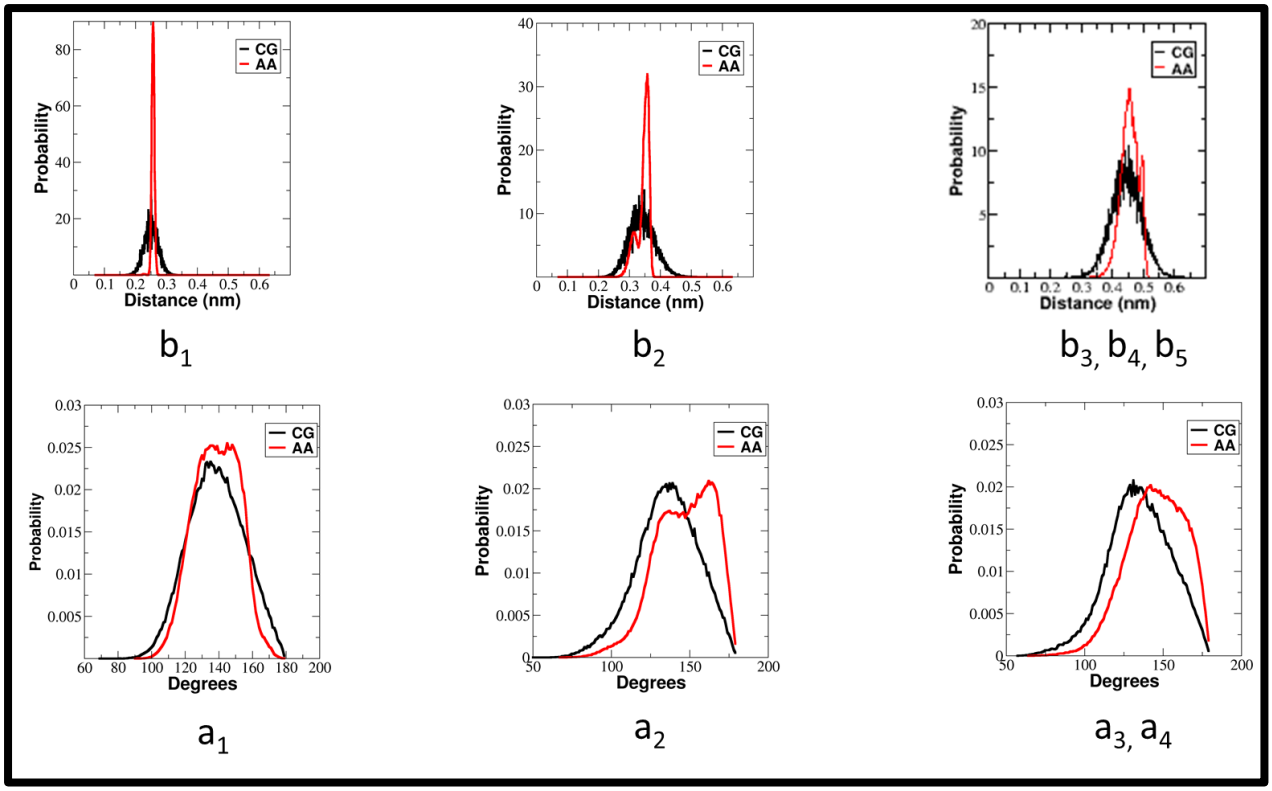


**Figure S4.** Bond and angle distributions for Isopropyl palmitate.

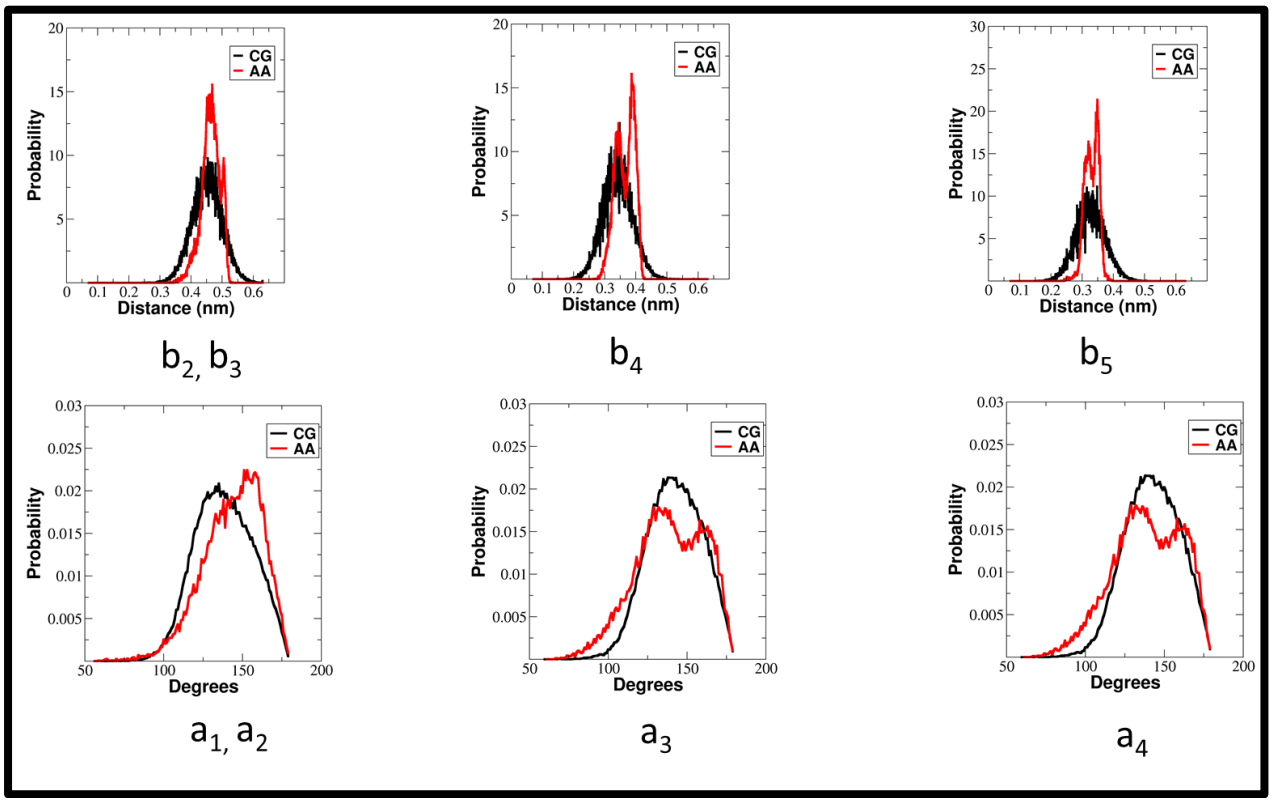


**Figure S5.** Bond and angle distributions for Monoolein

**Table S2.** Bonded parameters for molecules

| Geraniol | | | |
|---|---|---|---|
| | | | |
| | Bead types | $b_o$ (nm) | $K_b$ (KJ/mol nm$^2$) |
| b1 | P3-C2 | 0.350 | 1750 |
| b2 | C2-C3 | 0.420 | 1500 |
| | | $\theta_o$ (deg) | $K_\theta$ (KJ/ mol) |
| a1 | P3-C2-C3 | 130 | 15 |
| | | | |
| Geranic Acid | | | |
| | Bead types | $b_o$ (nm) | $K_b$ (KJ/mol nm$^2$) |
| b1 | P3-C1 | 0.350 | 1500 |
| b2 | C1-C1 | 0.400 | 1500 |
| | | $\theta_o$ (deg) | $K_\theta$ (KJ/ mol) |
| a1 | P3-C1-C1 | 130 | 15 |
| | | | |
| Isopropyl Palmitate | | | |
| | Bead types | $b_o$ (nm) | $K_b$ (KJ/mol nm$^2$) |
| b1 | SC2-P3 | 0.260 | 5000 |
| b2 | P3-C1 | 0.370 | 1250 |
| b3, b4, b5 | C1-C1 | 0.470 | 1250 |
| | | $\theta_o$ (deg) | $K_\theta$ (KJ/ mol) |
| a1 | SC2-P3-C1 | 138.56 | 25 |
| a2 | P3-C1-C1 | 160.00 | 15 |
| a3, a4 | C1-C1-C1 | 160.00 | 15 |
| | | | |
| Monoolein | | | |
| | Bead types | $b_o$ (nm) | $K_b$ (KJ/mol nm$^2$) |
| b2, b3 | C2-C2, C2-C1 | 0.475 | 1250 |
| b4 | C1-Na | 0.375 | 1250 |
| b5 | Na-P4 | 0.375 | 1250 |
| | | $\theta_o$ (deg) | $K_\theta$ (KJ/ mol) |
| a1, a2 | C1-C2-C2, C2-C2-C1 | 150 | 25 |
| a3 | C2-C1-Na | 140 | 15 |
| a4 | C1-Na-P4 | 125 | 25 |
| | | | |
| Limonene | | | |
| | Bead types | $b_o$ (nm) | $K_b$ (KJ/mol nm$^2$) |
| b1 | SC5-SC3 | 0.320 | 5000 |
| b2,b3,b4 | SC3-C5, SC3-SC4, C5-SC4 | 0.270 | constraint |
| | | $\theta_o$ (deg) | $K_\theta$ (KJ/ mol) |
| a1 | SC5-SC3-C5 | 150 | 50 |
| a2 | SC5-SC3-SC4 | 150 | 50 |
| | | $\varphi_o$ (deg) | $K_\varphi$ (KJ/mol) n |
| d1 | SC5-SC5-SC4-SC3 | 0.00 | 50.0 2 |
| | | | |

| Octyl Pyrrolidone | | | |
|---|---|---|---|
| | Bead types | $b_o$ (nm) | $K_b$ (KJ/mol $nm^2$) |
| b1 | C1-C1 | 0.47 | 2000 |
| b2 | C1-P3 | 0.25 | 1750 |
| b3 | P3-Na | 0.180 | constraint |
| b4 | P3-SNd | 0.230 | constraint |
| b5 | Na-SNd | 0.192 | constraint |
| | | $\theta_o$ (deg) | $K_\theta$ (KJ/ mol) |
| a1 | C1-C1-P3 | 180 | 20 |
| | | | |
| | | | |

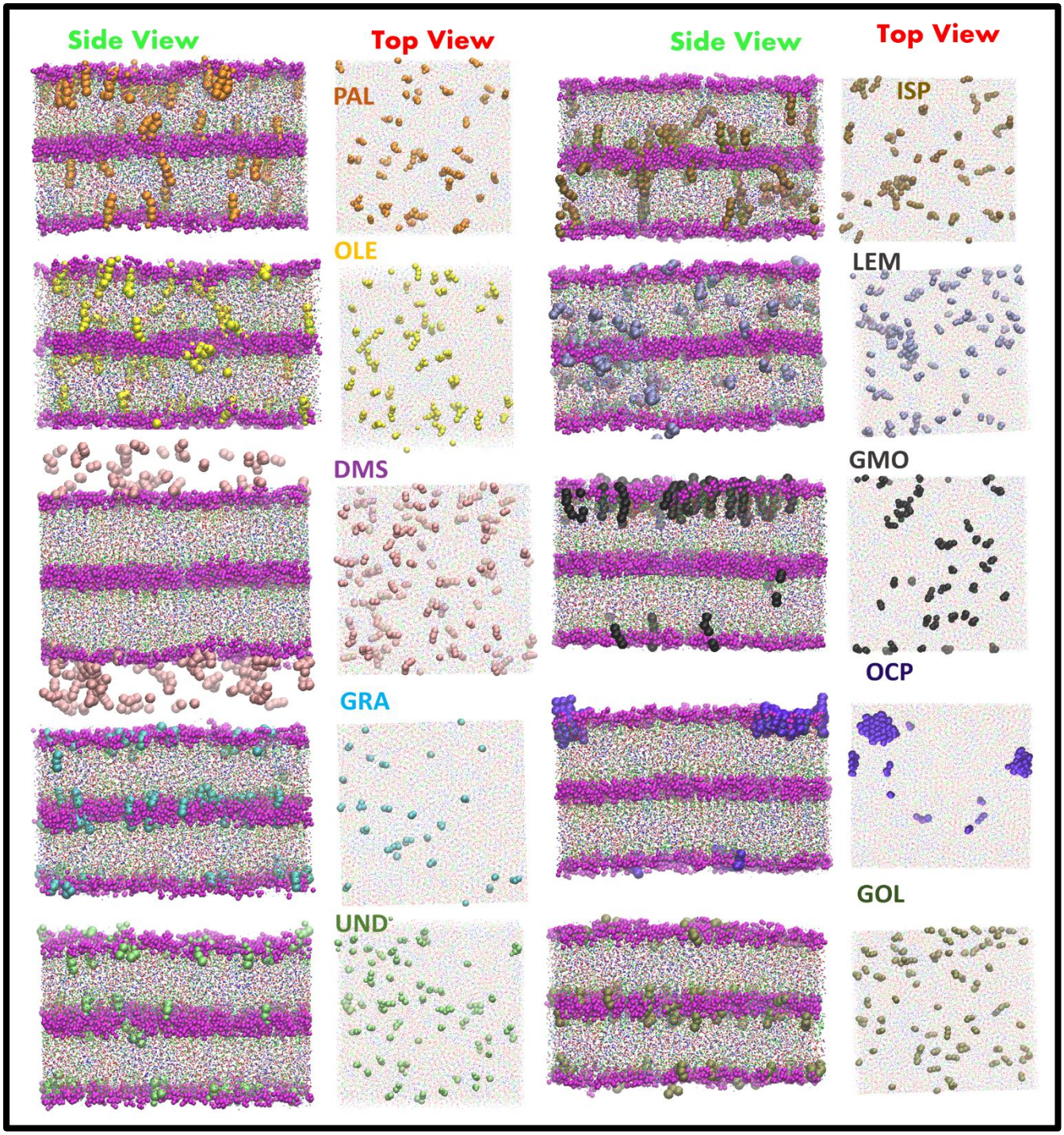


**Figure S6.** Snapshots of final configuration of skin double layer interacting with chemical permeation enhancers (at 3w/v concentration). Both side view (shows permeation of CPE's) and top view (shows dispersion or agglomeration of CPEs inside the layers) are shown. All systems were run for 3 μs. The skin lipid constituent CER, CHOL and FFA are shown (in point form of VMD software) in red, green and blue colors, respectively. The solvent (ethanol and water) are shown here. The permeation enhancers are shown in VDW form of VMD software.

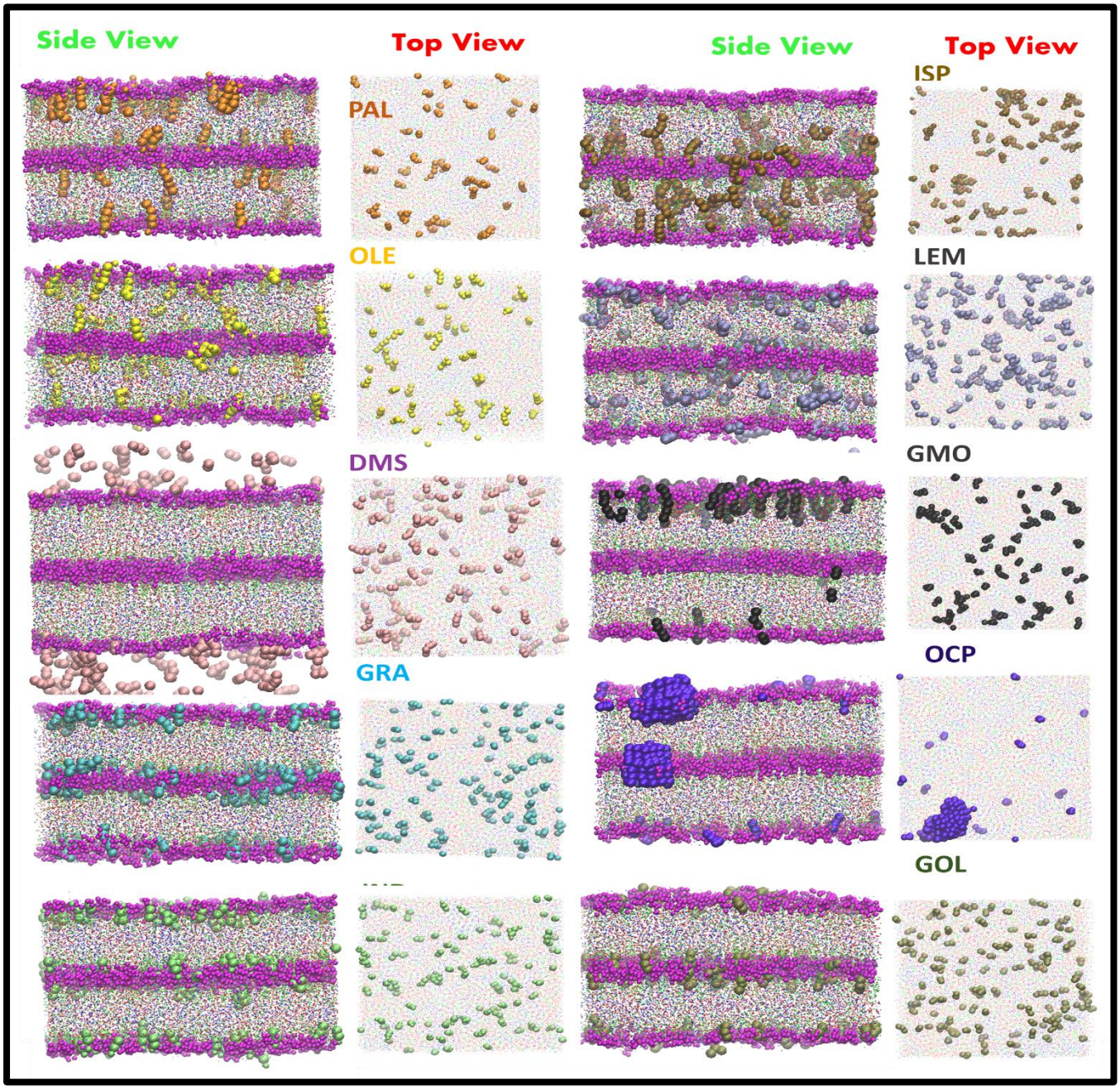


**Figure S7.** Snapshots of final configuration of skin double layer interacting with chemical permeation enhancers (at 5w/v concentration). Both side view (shows permeation of CPE's) and top view (shows dispersion or agglomeration of CPEs inside the layers) are shown. All systems were run for 3 μs. The skin lipid constituent CER, CHOL and FFA are shown (in point form of VMD software) in red, green and blue colors, respectively. The solvent (ethanol and water) are shown here. The permeation enhancers are shown in VDW form of VMD software.

## S3. Radial distribution function of CPEs

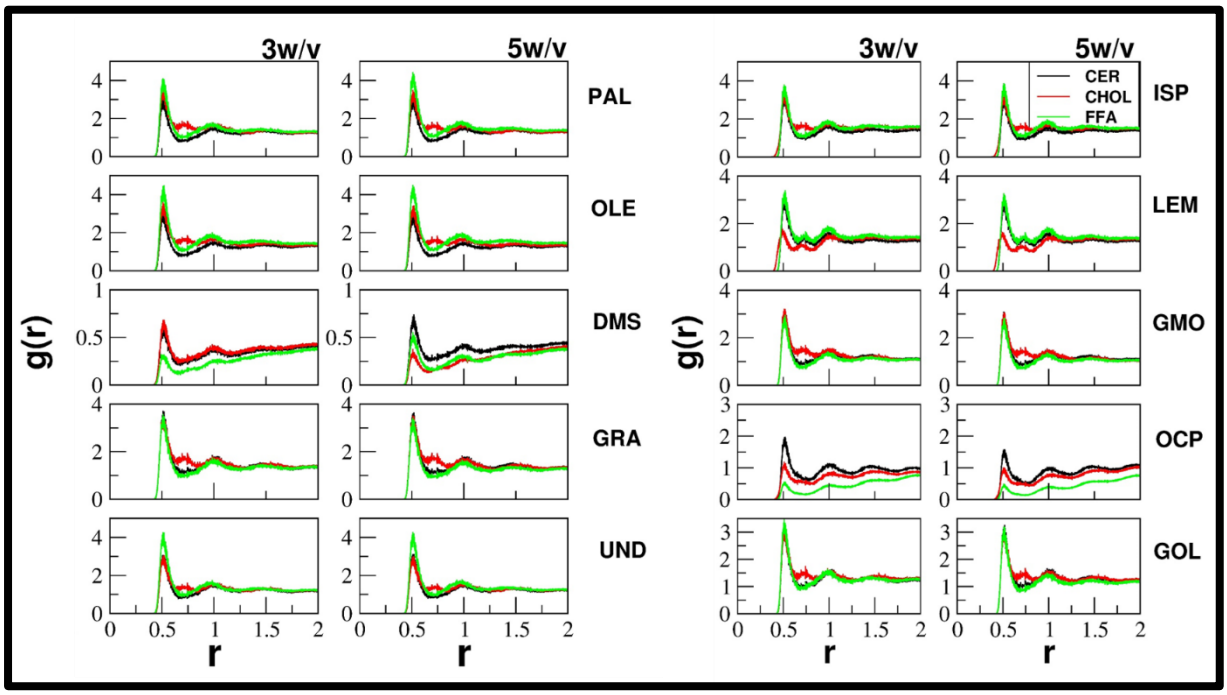


**Figure S8.** The radial distribution function g(r) of each permeation enhancer with skin lipid constituents (at 3 %w/v and 5 %w/v concentration), calculated in last 500 ns of production run. The peaks in g(r) profiles show the extent of the interaction between permeation enhancers and the particular lipid constituent.

## S4. Mean Square displacement of CPEs

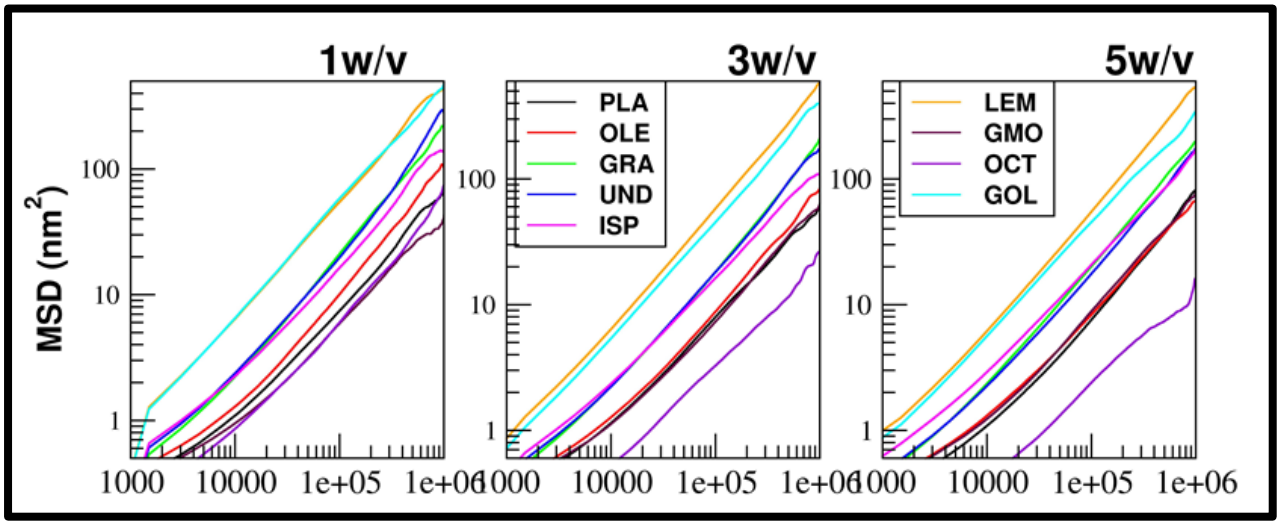


**Figure S9.** The mean square displacement of each permeation enhancers in skin lipid bilayer. The MSD was calculated in last 1 µs of production run.

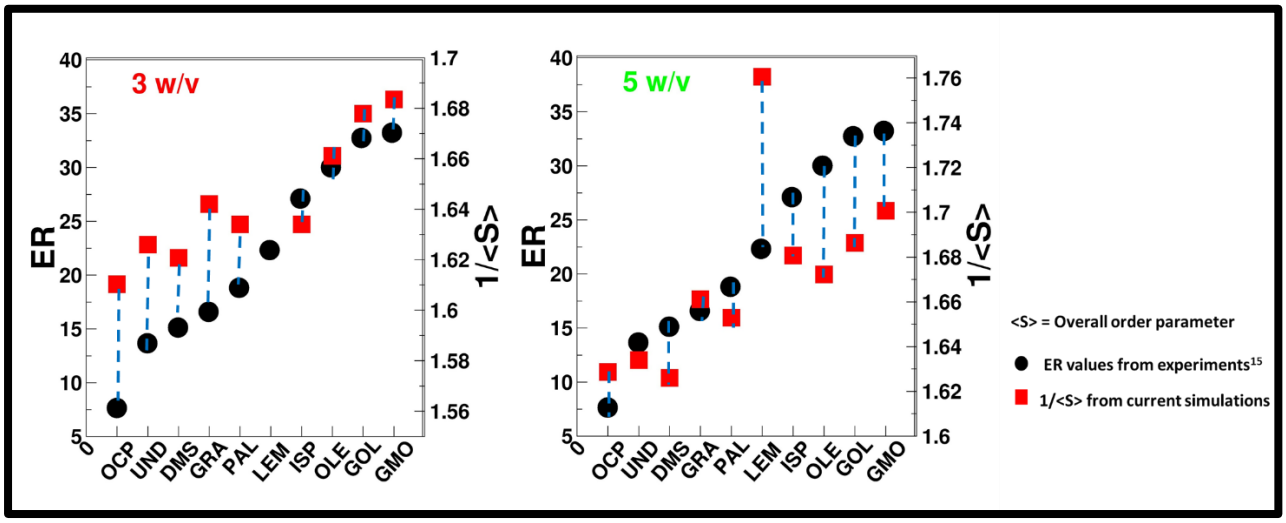


**Figure S10.** Comparison of experimental property enhancement ratio (ER) and the calculated property (1/<*S*>) from simulations for system 3%w/v and 5 %w/v. Both properties are plotted on different graphs due to the difference in the magnitude of each property.

References:

1. Monticelli, L., Kandasamy, S.K., Periole, X., Larson, R.G., Tieleman, D.P. and Marrink, S.J., 2008. The MARTINI coarse-grained force field: extension to proteins. Journal of chemical theory and computation, 4(5), pp.819-834

2. de Jong, D.H., Singh, G., Bennett, W.D., Arnarez, C., Wassenaar, T.A., Schäfer, L.V., Periole, X., Tieleman, D.P. and Marrink, S.J., 2012. Improved parameters for the martini coarse-grained protein force field. Journal of Chemical Theory and Computation, 9(1), pp.687-697.